

Non-Axisymmetric Field Generation within an Ambient Field

A. A. Darah¹

¹Department of Mathematics, Science Faculty, University of Alasmarya, Zliten, LIBYA

Abstract: The magnetic field of many astrophysical bodies is generated in the flow of electrically conducting fluid confirmed in a spherical shell, the flow is normally a threshold process, the dynamo requires motions of sufficient strength to overcome the innate magnetic diffusion. With presence of an ambient field, the requirement of strength of motion is not needed, and the magnetic field could be generated even for relatively weak flows we compute the non-axisymmetric magnetic field with imposed stationary and oscillatory external ambient magnetic field similar to Darah and Sarson 2007 which studied the axisymmetric magnetic field. The critical values of R_α do not needed to generate magnetic field. Many astrophysical objects exist within an external magnetic field of others, moons of Jupiter for example, lie within an external magnetic field of Jupiter Sarson et al. 1999. In this paper, the consideration is for the generation of magnetic field on a spherical mean-field $\alpha^2\omega$ dynamo model and the effect of an axial ambient field through nonlinear calculations with α - quenching feed back.

Keywords: mean-field dynamo; non-axisymmetric; nonlinear; ambient field.

I. Introduction

After many years of consideration, it is understood that the majority of astrophysical objects possess their magnetic field which is generated by hydromagnetic dynamo (HMD) dynamo process, in this process, the motion of electrically conducting fluid in the presence of basic mechanisms generates an electrical current which produces the magnetic field in the core Levy 1979, Gubbins 2000. The basic mechanism is responsible for such self-excited dynamo action Fearn 2004. The generative magnetic field is threshold process terms of the fluid velocity, so the magnetic field to be generated requires that the velocity exceeds some critical values Levy 1979.

The generated magnetic fields could be axisymmetric in some objects as the field of the Earth, Saturn, non-axisymmetric as the field of the Sun or mixed of axisymmetric and non-axisymmetric field, Starchenko 1993, which will be in future work. During the study, most work has focused on the axisymmetric magnetic field, the reason for that, may be, because it is easier to excite than the non-axisymmetric field. There have been some studies on non-axisymmetric dynamo models. The possibility of non-axisymmetric modes has first been investigated by Stix 1971, Krause 1971, Roberts & Stix 1972 and Ruzmaikin et al. 1988 for $\alpha\omega$ -dynamo. And Rädler 1975 for α^2 -dynamo Sarson et al. 1997, Moss 1999 obtained stable solutions that produced a small non-axisymmetric field component. Bigazzi & Ruzmaikin 2004 studied the generation of non-axisymmetric field and their coupling with axisymmetric solar magnetic field.

Some of astrophysical objects exist within an external field of others. In our universe, many of moons lie within the field generated by the giant planets. The possibility of the Jovian field influencing the MHD processes of the Galilean moons Levy 1979. The larger moons of Saturn are also lie within the background field produced by Saturn, moons of Jupiter; Io, Europa, Ganymede and Callisto, lie within the magnetic field generated by the dynamo action of Jupiter Kivelson et al. 1996. Similar situations for stellar dynamo within binary system. Several authors studied galactic and accretion disc dynamos within external fields (e.g. Moss & Shukurov 2001, 2004).

Data from Galileo orbiter indicated that, the two of Jupiter's moons; Io and Ganymede, have significant magnetic fields of internal, these fields are produced by some form of MHD processes, similar to the mechanism thought to be responsible for the magnetic field of the Earth and other terrestrial planets. However, that happens within the magnetic field of Jupiter. The ambient magnetic field that the Jovian moons experience has contributions from Jupiter's intrinsic field and from the field of a plasma sheet in the Jovian magnetosphere.

In this case the generation of magnetic field does not need critical values of ω or α -effects. The Jovian magnetic field is non-axisymmetric, it rotates with the planet in a time scale much faster than of the internal MHD processes and so the relevant contribution to the ambient field is the Jovian field time-averaged over a Jupiter rotation.

Io and Ganymede have dipole moments of about equal strength; they lie, however, in ambient fields of different strength (Kivelson et al. 1996). It is possible that Io and Ganymede generate magnetic fields by their dynamo processes with ambient field of secondary.

The presence of the ambient field admits a second possibility, however; that the differing ratios of imposed field to intrinsic field are significant, and that the two moons operate in quite different MHD regimes, the MHD processes dominated by the ambient field, may be important in the case of Io (Schubert et. al. 1996). The intrinsic field of terrestrial planets produced within the core of object is much stronger than the ambient field but the relatively weak ambient field should help toward the generation of magnetic fields. Our investigation is concerned on the situation of the planets which effected with ambient fields as Jupiter’s moons.

We studied some cases of the generation of magnetic fields using different values of R_ω and R_α effects. The work presented here is similar to Darah and Sarson 2007, but this work is focusing on the nonaxisymmetric mean field dynamo within an axial external field (either constant, or harmonically oscillating), we consider different regimes of interaction between simple dynamo systems and a fluctuating external field of varying strength. We consider a spherical shell geometry, similar to that of the Earth, but the conclusion will not be widely different for Earth-like problems.

We assume the fluid motion (and α -effect) is symmetric (antisymmetric) about the equatorial plane. The magnetic field may then also be of ‘pure’ symmetry — either dipole (antisymmetric) or quadrupole (symmetric) about the equator — or of ‘mixed’ symmetry (see, e.g. Gubbins & Zhang 1994). Here we consider the possibility of solutions of each symmetry type; indeed, the possibility of the (dipole) external field influencing the solution symmetry is one of the most interesting aspects of the problem, from the theoretical viewpoint.

II. Model

Most of studies have been done, so far, were concerned with the axisymmetric model, Barengi 1993, Hollerbach & Jones 1993 however, the magnetic field occurring in physical systems is not necessarily to be axisymmetric but may well be non-axisymmetric with respect to the rotation axis. And it can be symmetric or antisymmetric about the equatorial plane. The first investigations of non-axisymmetric $\alpha\omega$ dynamos were by Krause 1971, who pointed out that symmetric fields in the non-axisymmetric model have smaller eigenvalues than the antisymmetric fields on the α -effect dynamo, and also studied by Roberts & Stix 1972. So

this paper will be concerned with non-axisymmetric magnetic fields. We will consider the induction equation for a single non-axisymmetric wave-number in our spherical shell model; first, with no ambient magnetic field, and then with an ambient magnetic field of nonaxisymmetric geometry in the form of an equatorial dipole.

The system consists of an electrically conducting fluid contained in a spherical shell, and the region interior to the fluid is finitely conducting, and is of the same conductivity as the fluid itself.

\mathbf{U} , \mathbf{b}^i and \mathbf{b}^o are fluid flow and inner and outer core magnetic fields respectively, and \mathbf{b}_1 is an ambient magnetic field.

The non-axisymmetric equations are

$$\frac{\partial \mathbf{b}^i}{\partial t} = \nabla^2 \mathbf{b}^i, \quad (1)$$

$$\nabla \cdot \mathbf{b}^i = 0, \quad (2)$$

for inner core magnetic field \mathbf{b}^i ; and

$$\frac{\partial \mathbf{b}^o}{\partial t} = \nabla \times [\mathbf{U} \times (\mathbf{b}^o + \mathbf{b}_1) + \nabla \times \alpha(\mathbf{b}^o + \mathbf{b}_1)] + \nabla^2 \mathbf{b}^o, \quad (3)$$

$$\nabla \cdot \mathbf{b}^o = 0. \quad (4)$$

for outer core magnetic field \mathbf{b}^o , e.g., Hollerbach & Jones (1993). The decomposition of the nonaxisymmetric field into toroidal and poloidal parts is

$$\mathbf{b} = \nabla \times (g \hat{\mathbf{e}}_r) + \nabla \times \nabla \times (h \hat{\mathbf{e}}_r) \quad (5)$$

The flow \mathbf{U} and α -effect are axisymmetric, we assumed, as e.g., Brandenburg et al. (1989), a functional form for α given by

$$\alpha = \frac{\alpha_0 \cos \theta}{1+b^2}, \quad (6)$$

Where α_0 is a constant.

The equations are non-dimensionalised using the length-scale of the shell, $\mathcal{L} = r_o - r_i$, where r_o and r_i are the outer and inner core radii, and the magnetic diffusion time-scale, $\mathcal{T} = \mathcal{L}^2/\eta$ where η is the magnetic diffusivity. This leaves the mean-field equations governed by the non-dimensional parameters

$$R_\omega = \frac{\omega_0 \mathcal{L}^2}{\eta}, \quad R_\alpha = \frac{\alpha_0 \mathcal{L}^2}{\eta}. \quad (7)$$

In the following, we will fix R_ω , and treat R_α as our control parameter. The radius ratio $\frac{r_i}{r_o} = 1/3$ is adopted. (This value is approximately that applicable to the Earth, here considered a model for other terrestrial planets.)

The variables g, h , are expanded in the outer core, e.g., Jones et al. 1995, as

$$g^o = \sum_{n=1}^N \sum_{l=1}^{M+2} g_{nl}^o T_{l-1}(x_o) P_j^{(m)}(\cos \theta) e^{im\phi}, \quad (8)$$

$$h^o = \sum_{n=1}^N \sum_{l=1}^{M+2} h_{nl}^o T_{l-1}(x_o) P_j^{(m)}(\cos \theta) e^{im\phi}, \quad (9)$$

and in the inner core as

$$g^i = \sum_{n=1}^N \sum_{l=1}^{\frac{M}{2}+1} g_{nl}^i T_{2l-1}(x_i) P_j^{(m)}(\cos \theta) e^{im\phi}, \quad (10)$$

$$h^i = \sum_{n=1}^N \sum_{l=1}^{\frac{M}{2}+1} h_{nl}^i T_{2l-1}(x_i) P_j^{(m)}(\cos \theta) e^{im\phi}, \quad (11)$$

where $x_o = 2(r - r_i) - 1$ is the radial coordinate normalized to $(-1, 1)$, and $x_i = r/r_i$. $k_1 = 2, k_2 = 1$ for even m and $k_1 = 1, k_2 = 2$ for odd m to obtain the dipole components; and $k_1 = 1, k_2 = 2$ for even m and $k_1 = 2, k_2 = 1$ for odd m for the quadrupole components.

$P_n^m(\cos \theta)$ are the associated Legendre functions, $T_l(x)$ are Chebyshev polynomials. The truncation which has been used in this work is $M = 12$ and $N = 6$. Some checks of the system have been made at a higher truncations ($M = 16, 20$ and $N = 8, 10$, respectively) figure 1, however.

j is replaced by $(2n + m - 2)$ in the equations (8) and (10), and by

$(2n + m - 1)$ in the equations (9) and (11) to obtain the dipole model. For the quadrupole model j will be replaced by $(2n + m - 1)$ in equations (8) and (10) and by $(2n + m - 2)$ in equations (9) and (11). The mixed system j includes both dipole and quadrupole components. In this work we consider only the case $m = 1$, however.

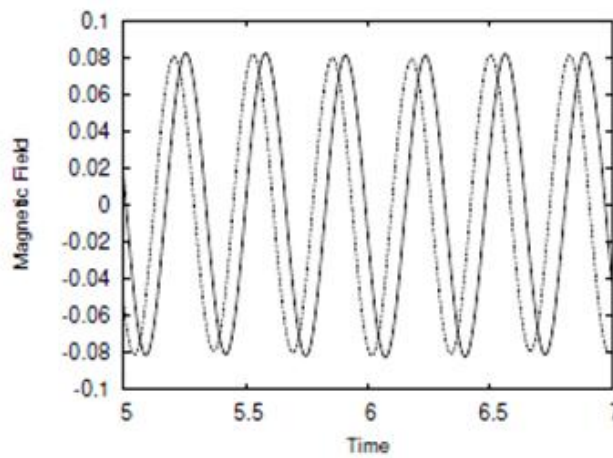


Figure 1: The magnetic field for truncations ($N=6, M=12$) solid line and ($N=8, M=16$) dashed line.

The ambient magnetic field \mathbf{b}_1 can be written as

$$\mathbf{b}_1 = \nabla \times \nabla \times (h_1 \hat{\mathbf{r}}), \quad (12)$$

where

$$h_1 = b_1 h_1(r) P_1^1(\cos \theta) e^{i\phi}, \quad (13)$$

and

$$h_1(r) = -\frac{1}{2} r^2. \quad (14)$$

Within the code, $h_1(r)$ is expanded as a Chebyshev series, as

$$h_1(r) = \sum_{l=1}^3 h_{1l}^o T_{l-1}(x_o), \quad (15)$$

in the outer core, with

$$h_{1,1}^o = -9/16, h_{1,2}^o = -1/2, \text{ and } h_{1,3}^o = -1/16, \text{ and as}$$

$$h_1(r) = h_{1,1}^i x_i T_{2i-1}(x_i), \quad (16)$$

in the inner core, with

$$h_{1,1}^i = -1/8.$$

The boundary conditions on the magnetic field are derived from matching the outer and inner fields at $r = r_i$ and matching the outer field to the field in an insulator at $r = r_o$.

This gives, for the poloidal field:

$$h^i = h^o, \quad \frac{\partial h^i}{\partial r} = \frac{\partial h^o}{\partial r}, \quad \text{at } r = r_i \quad (17)$$

and the toroidal field:

$$g^i = g^o, \quad \frac{\partial g^i}{\partial r} = \frac{\partial g^o}{\partial r}, \quad \text{at } r = r_i \quad (18)$$

$$g^o = 0, \quad \text{at } r = r_o \quad (19)$$

The coefficients for the model quantities are all complex with the physical variables being the real part of the quantity, e.g.

$$\Re(h e^{im\phi}) = \Re(h) \cos m\phi - \Im(h) \sin m\phi. \quad (20)$$

The background field will be allowed to vary in time, in the form of a rotating equatorial dipole. This then takes the form

$$h_1 = b_1 h_1(r) P_1^1(\cos \theta) e^{i\phi} e^{i\nu_1 t}, \quad (21)$$

$$= b_1 h_1(r) P_1^1(\cos \theta) e^{i(\phi + \nu_1 t)}, \quad (22)$$

with the physical field being given by the real part, as before. Here, ν_1 is the rotation frequency of the imposed field.

III. Results

In presenting the non-axisymmetric results, we treat the solutions in three categories. First the calculation with no background magnetic field ($b_1 = 0, \nu_1 = 0$). Then, the results with a constant ambient magnetic field ($b_1 \neq 0$, constant) and $\nu_1 = 0$. Finally, the results with an oscillating external magnetic field ($b_1 \neq 0, \nu_1 \neq 0$).

The description of the solutions types illustrated in the table 1.

Code	Solution	Code	Solution
D	Dipole	S	Stationary
Q	Quadrupole	O	Oscillatory
M	Mixed	R	S. En. & O. Fi

Table 1: Codes for the different types of solutions of magnetic Energy and magnetic Field

By testing the system for different values of R_ω , it's appeared that the more interesting values are accrued at $R_\omega > 20$, and according to the paper (Darah & Sarson), which studied the axisymmetric magnetic field generation within an ambient field at $R_\omega = 25, 50$ and 100 , so we carried out the calculation with the same values of R_ω .

2.1 No ambient field ($b_1 = 0$)

Firstly, we fix $R_\omega = 25$ and vary R_α . The onset of dynamo action is at $R_{ac} \cong 7$, where the solution is *SD*. At a bifurcation value $R_{ab} \geq 8.3$, it becomes *OM* with two frequencies for the magnetic field and also two frequencies for the magnetic energy, and remains the same up to $R_{ac} \cong 38$ where it becomes *RQ* (Figure 2). For example, at $R_\alpha = 20$, the solution has an oscillatory magnetic energy frequencies 15 and 36 and magnetic field behaviour with frequencies 18 and 33 (Figure 3), whereas at $R_\alpha = 60$ — where the solution has a stationary energy behavior — the magnetic field has an oscillatory behaviour with a frequency 20 (Figure 4), corresponding to rotation of internal field. These solutions are illustrated in figure 5.

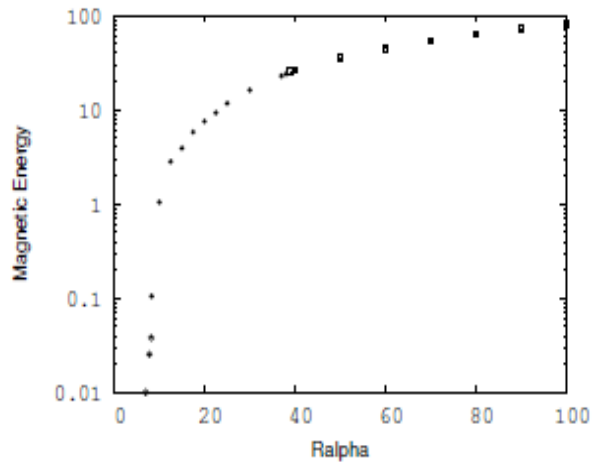


Figure 2: The total energy SD (open circles) for $R_\alpha < 8.3$, OM (closed circles) for $8.3 < R_\alpha < 38$ and SQ (squares) for $R_\alpha > 38$ of the non-axisymmetric solutions for $R_\omega = 25$ and $b_1 = 0$.

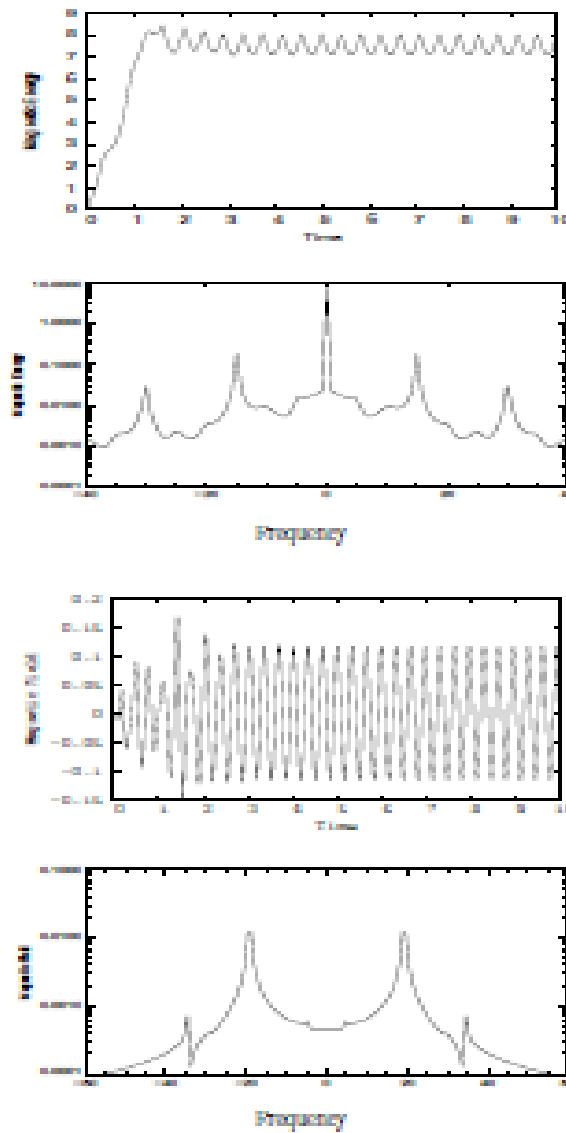


Figure 3: The total magnetic energy and its corresponding Fourier transform (the first and second rows) respectively

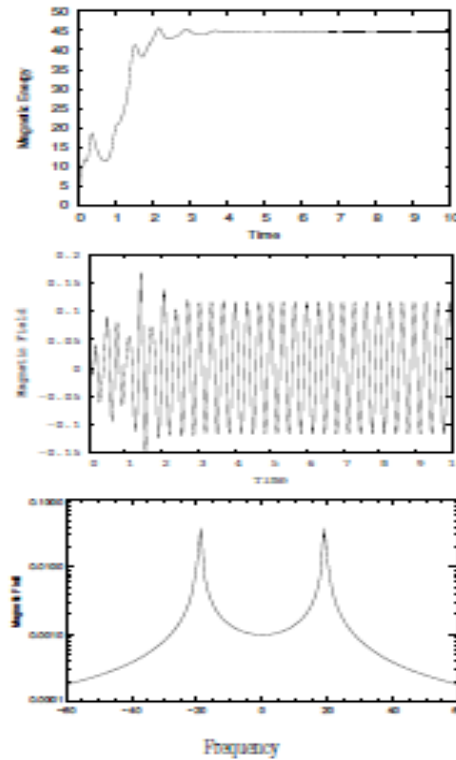


Figure 4: The total magnetic energy (top) and the total magnetic field and its corresponding Fourier transform (the middle and bottom) respectively of the nonaxisymmetric solution at $R_\omega = 25, R_\alpha = 60$ and $b_1 = 0.0$

And the magnetic field and its corresponding Fourier transform (the third and fourth rows) respectively, of the non-axisymmetric solution at $R_\omega = 25, R_\alpha = 20$ and $b_1 = 0.0$.

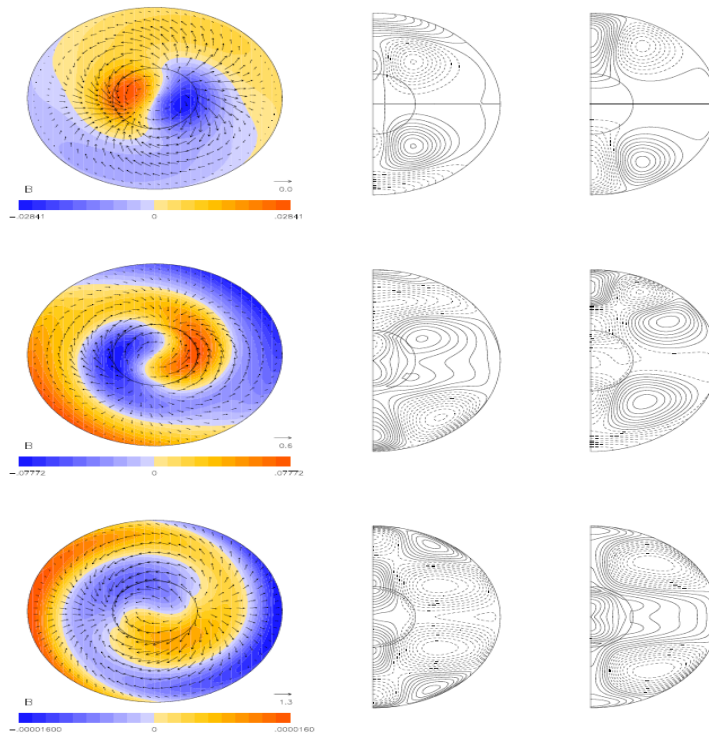


Figure 5: The behavior of the magnetic field at $z = 0.0$ (first column), $\phi = 0$ (second column) and $\phi = 90$ (third column) for the nonaxisymmetric magnetic field at $R_\omega = 25, b_1 = 0.0$ and $R_\alpha = 7.6$ (first row), $R_\alpha = 20$ (second row) and $R_\alpha = 60$ (third row). The contours in the second and third columns show azimuthal field B_ϕ .

Secondly, for $R_\omega = 50$, there are actually two solution branches: the first is an *OD*, it starts to act as a dynamo at $R_\alpha \cong 9$. The second branch is an *OM*, it appears at $R_\alpha \cong 15$, the solutions at $R_\alpha \cong 10$ for example, has an *OD* behaviour with a magnetic field frequency 18, and another solution appears at $R_\alpha = 20$, the solution has an *OM* behaviour with a magnetic field frequency 29 (Figure 6). At $R_\alpha = 30$, both solutions become chaotic.

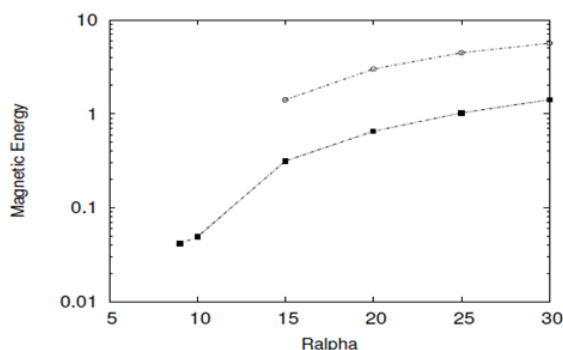


Figure 6: The magnetic energy of the dipole solution (squared line) and the mixed solution (circle line) for non-axisymmetric solutions at $R_\omega = 50$ and $b_1 = 0$.

Finally, for $R_\omega = 100$ the solution has a consistent *OQ* behaviour, with an onset value for dynamo action at $R_\alpha \cong 10$ (Figure 7) see also (Figure 8).

At $R_\alpha \cong 50$, the solution has an oscillatory magnetic field behavior with a frequency 55. Table (2) summarises the critical values $R_{(\alpha,c,b)}$ for the various values of R_ω .

R_ω	$R_{(\alpha,c,b)}$	Behaviour
25	7	<i>SD</i>
25	8.3	<i>OM</i>
25	38	<i>SQ</i>
50	9	<i>OD</i>
50	15	<i>OM</i>
50	10	<i>OQ</i>

Table 2: R_ω and the corresponding $R_{(\alpha,c,b)}$ critical and bifurcations values.

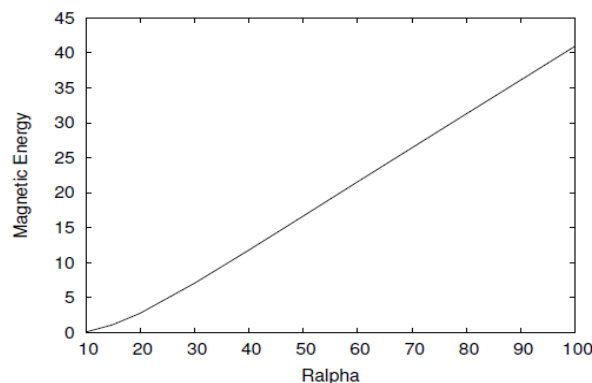


Figure 7: The quadrupole oscillatory solution of the magnetic energy for $R_\omega = 100$ and $b_1 = 0$.

2.1 Constant ambient field ($b_1 \neq 0$ and $v_1 = 0$)

From the preceding section we can see that the more interesting solution occurs at $R_\omega = 25$. At this value we could not only more than one solution behaviour, but also the solutions seem to be consistent *OQ* even for $R_\alpha \cong 100$. So we carry out the calculations with an ambient magnetic field present for this value of R_ω .

Fields are now generated even at $R_\alpha = 0$, and the critical values of R_α are not needed in this situation. For ambient magnetic fields with $b_1 = 0.1$ and 1.0 , the solutions start as *SQ* with energy values 0.0225 and 2.25 respectively. This energy corresponds to the constant energy of the ambient magnetic field, throughout the spherical shell and inner core. In fact, the magnetic energy E_m could be calculated as

$$E_m \cong \frac{1}{2} b_1^2 \int_V dV \quad (23)$$

$$\cong \frac{1}{2} b_1^2 \left(\frac{4}{3} \pi r_0^2\right) (24)$$

where V is the spherical volume.

At $R_{\alpha b} \cong 7$ the solution with $b_1 = 0.1$ becomes OQ , whereas the solution with $b_1 = 1.0$ becomes OQ at the bifurcation point $R_{\alpha b} \cong 11.5$ (Figure 10). At larger values of R_α , the solution with $b_1 = 0.1$ becomes stronger than with $b_1 = 1.0$, the ambient field acts somewhat to hinder dynamo action. At $R_\alpha = 20$, they have oscillatory solutions. The solution with $b_1 = 0.1$ has magnetic field frequencies 18 and 33 and magnetic energy frequencies 15 and 30 whereas, the solution with $b_1 = 1.0$ has 18 and 36 for both the magnetic energy and the magnetic field frequencies (Figure 9). Here the frequency $\nu_1 = 18$ is the natural frequency ν_n in this case, we use this value in the following sections. It has a negative sign corresponding to clockwise direction rotation.

2.2 Rotating ambient field ($b_1 \neq 0$ and $\nu_1 \neq 0$)

The calculations in this section are concerned with the system with $R_\omega = 25$ and $b_1 = 1.0$. From the previous, the model with $\nu_1 = 0$ has two solution types: stationary at $R_\alpha < 11.5$, and oscillatory at $R_\alpha > 11.5$. So we considered the two values $R_\alpha = 10, 20$. For the former value, the solution is “stationary”, for the latter value the solution is “oscillatory”. First, we fix $R_\omega = 25$, $R_\alpha = 20$, $b_1 = 1.0$ and vary $\nu > 0$. We know from the preceding section that the model with $\nu_1 = 0$ has an OQ with a natural frequency $\nu_n \cong 18$. The calculation shows that the solutions have similar OQ behaviour even for $\nu_1 \gg \nu_n$. The effect of increasing ν_1 is that the magnetic energy frequency (ν) increases with ν_1 and it equals $\nu = \nu_1 + \nu_n$. Table 3 shows some values of the ν_1 and the corresponding solution frequencies $\nu = \nu_1 + \nu_n$.

Figure 11 and 13 show the behaviour of three solutions: magnetic energy is plotted vs time and, figure 12 and 14 vs the corresponding frequency respectively.

The behaviours seem to be similar OQ , but the frequency increases with ν_1 .

The frequency components of the magnetic energy can be understood by considering the interaction of two frequencies of rotation, ν_1 and ν_n . Then

$$b_x = b_1 \cos(\nu_1 t) + b_2 \cos(\nu_n t + \psi), \quad (25)$$

$$b_y = -b_1 \sin(\nu_1 t) - b_2 \sin(\nu_n t + \psi), \quad (26)$$

for some phase difference ψ , where b_1 and b_2 are real. The energy then goes as

$$E_m = b_1^2 + b_2^2 + b_1 b_2 \cos[(\nu_1 - \nu_n)t - \psi]. \quad (27)$$

So the signal in the time series of the energy have frequency $\nu_1 - \nu_n$.

ν_1	ν_n
0	18
1	19
15	33
30	48
100	118

Table 3: ν_1 and the corresponding magnetic energy frequencies ν at $R_\omega = 25$, $R_\alpha = 20$ and $b_1 = 1.0$.

Another interesting type of solutions occur, however, if ν_1 is further increased ($\nu_1 \gg \nu_n$). At $\nu_1 = 100$ for instance, the solution has two types of behaviour: an internal magnetic field and a skin magnetic field. Figure 15 shows the two types rotate at different speeds; between 15(A) and 15(C), the skin field has done one rotation in time $t \cong T_1$, and from 15(A) to 15(D) the interior field has done half a rotation in time $t \cong T_n$, where $T_k = 2\pi/\nu_k$ is period associated with the relevant frequency. Secondly, for $R_\omega = 25$, $R_\alpha = 10$ and $b_1 = 1.0$, the model at these parameters with $\nu_1 = 0$ has a SQ solution. At $\nu_1 = 1$ the magnetic energy is still stationary, but the magnetic field has an oscillatory behaviour with a frequency 1, and the solution has internal rotation in the ϕ direction; ie, the solution is RQ . By slightly increasing ν_1 , the magnetic energy becomes OQ at $\nu_1 \cong 5$ with a magnetic field frequency 5. This frequency increases with ν_1 . Figure 16 shows the magnetic energy vs time. The top solution is stationary ($\nu_1 = 1$), whereas the next two solutions are similar (oscillations), they are at $\nu_1 = 10$ and 100 and their magnetic energy frequencies are 28 and 108 respectively (Figure 17). At high value of $\nu_1 = 100$, the solution has a similar behavior to the solution at $R_\alpha = R_- = 20$ (Figure 18).

Figure 18 presents magnetic field behavior of the non-axisymmetric solution at $R_\omega = 25$, $R_\alpha = 10$ and $b_1 = 1.0$ and $\nu_1 = 100$ at times $t = 10.36, 10.42, 10.72$ (from top to bottom). The field has a double rotation behavior; the internal and boundary fields rotate at different speeds. The outer field has done one rotation in time $\delta_t \cong T_1$ (between first and second rows), whereas the inner field has done half a rotation in time $\delta_t \cong T_n/2$ (between first and third rows).

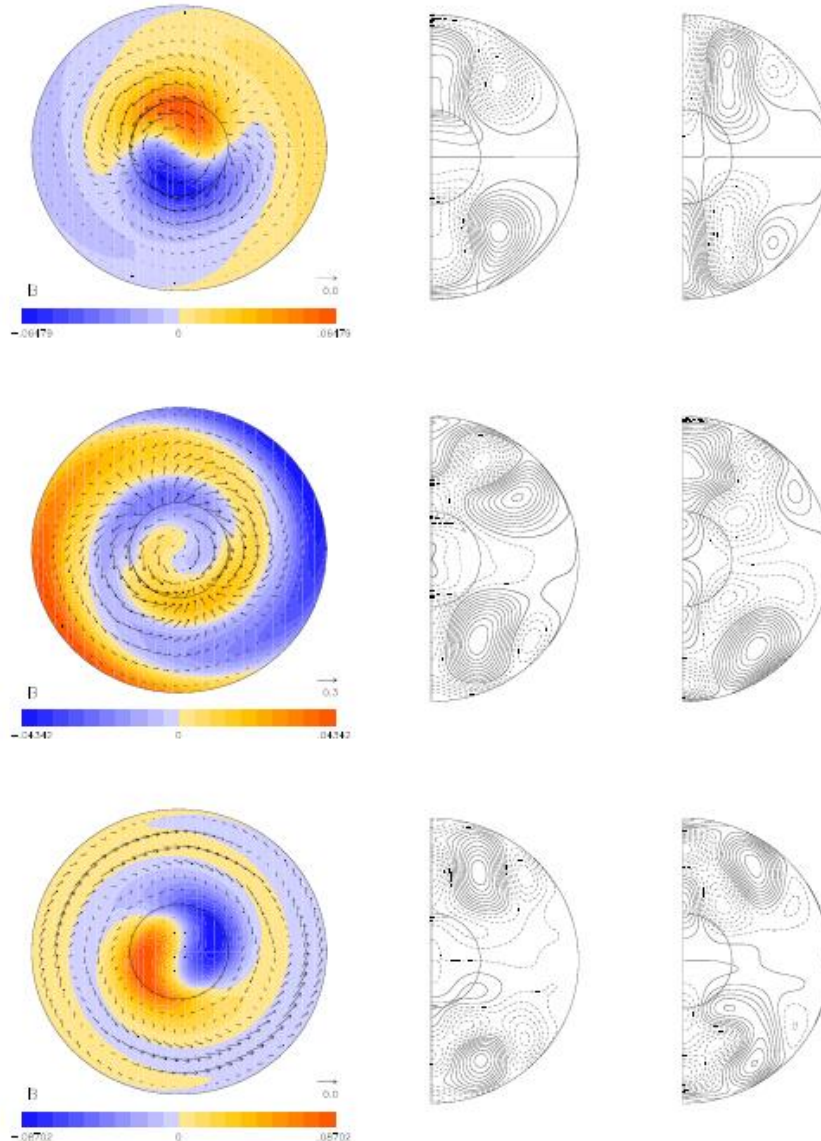


Figure 8: The behavior of the magnetic field at $z = 0.0$ (first column), $\phi = 0$ (second column) and $\phi = 90$ (third column) for $b_1 = 0.0$. the first and second rows illustrate the dipole and mixed solutions at $R_\omega = 50$ for $R_\alpha = 10$ and 20 , respectively, the third row is the quadrupole solution at $R_\omega = 100$ ($R_\alpha = 20$).

IV. Concluding Remarks

Three values of R_ω have been used in our calculations for the non-axisymmetric system: $R_\omega = 25, 50$ and 100 . The system has critical values of dynamo numbers. The solutions start as stationary (at $R_\omega = 25$) or oscillatory (at $R_\omega = 50$ and 100). The solution at $R_\omega = 50$ has two branches (OD and OM) with different critical R_α values, at $R_\alpha = 30$ both become chaotic. At $R_\omega = 100$, the system has consistent (OQ) solution with critical value of $R_\alpha = 10$. The more interesting solution occurs at $R_\omega = 25$ where it has three types of solution behaviors: SD , OM and RQ , with three transition values. Each of these solutions has oscillatory magnetic energy and magnetic field, corresponding to a rotation in the ϕ direction, except the case at $R_\omega = 25$ and $7 \leq R_\alpha < 8.3$, where the solution is SD . For the system with an ambient field ($b_1 \neq 0$), the more interesting solution occurs at $R_\omega = 25$ and $R_\omega = 100$. Since field is generated even at $R_\alpha = 0$, the solutions start as stationary or rotating until the first bifurcation point of R_α , where the solutions become (OQ). These bifurcation values increase with the external field b_1 value. For $R_\alpha > 7$ the magnetic energy at $b_1 = 0.1$ becomes larger than at $b_1 = 1.0$ as the ambient field inhibits the internal generation. Both solutions have their own magnetic energy and magnetic field frequencies.

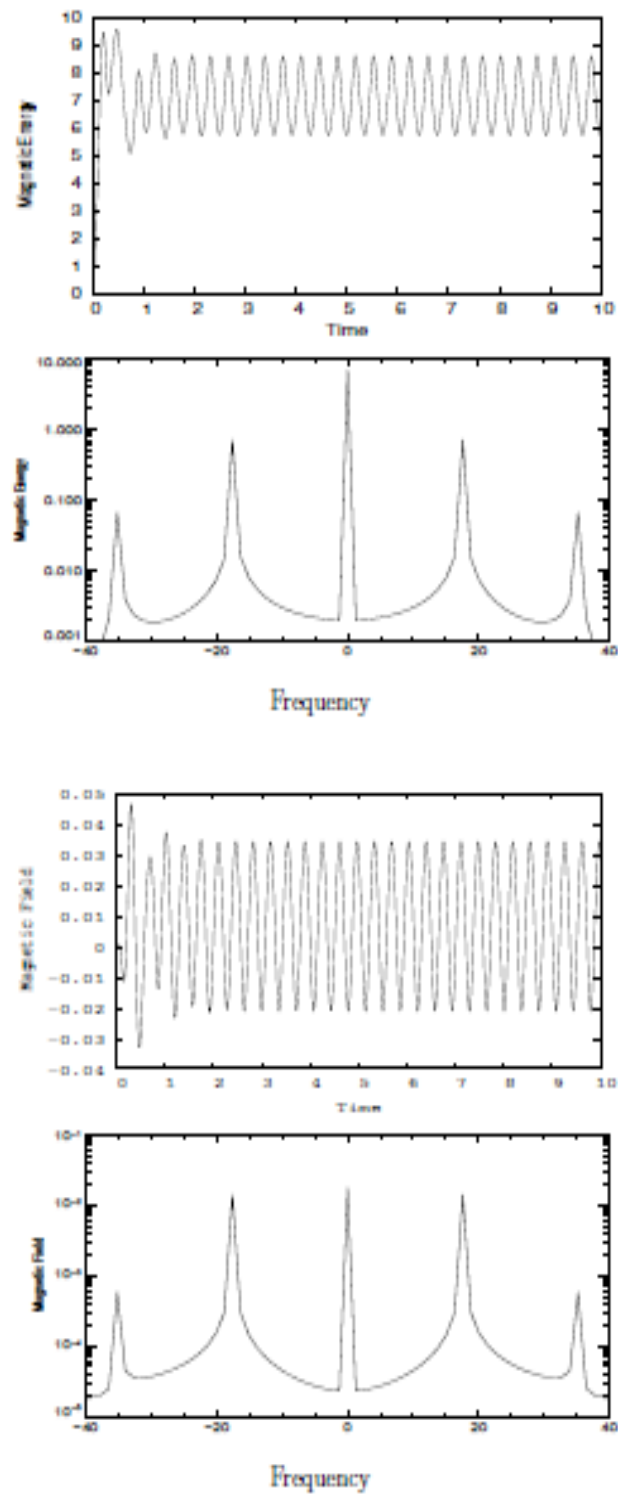


Figure 9: The magnetic energy and its Fourier transforms energy (top), and the magnetic field and its Fourier transforms (bottom) of the non-axisymmetric solution at $R_\omega = 25$, $R_\alpha = 20$ and $b_1 = 1.0$.

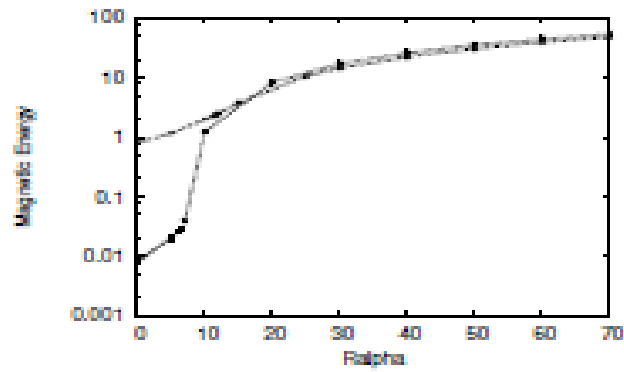


Figure 10: The magnetic energy of the quadrupole oscillatory solution for $R_\omega = 25$. At $b_1 = 0.1$, stationary (squared line) then oscillatory (stared line) solutions are shown; at $b_1 = 1.0$, stationary (dotted line) then oscillatory (circle line) solutions occur.

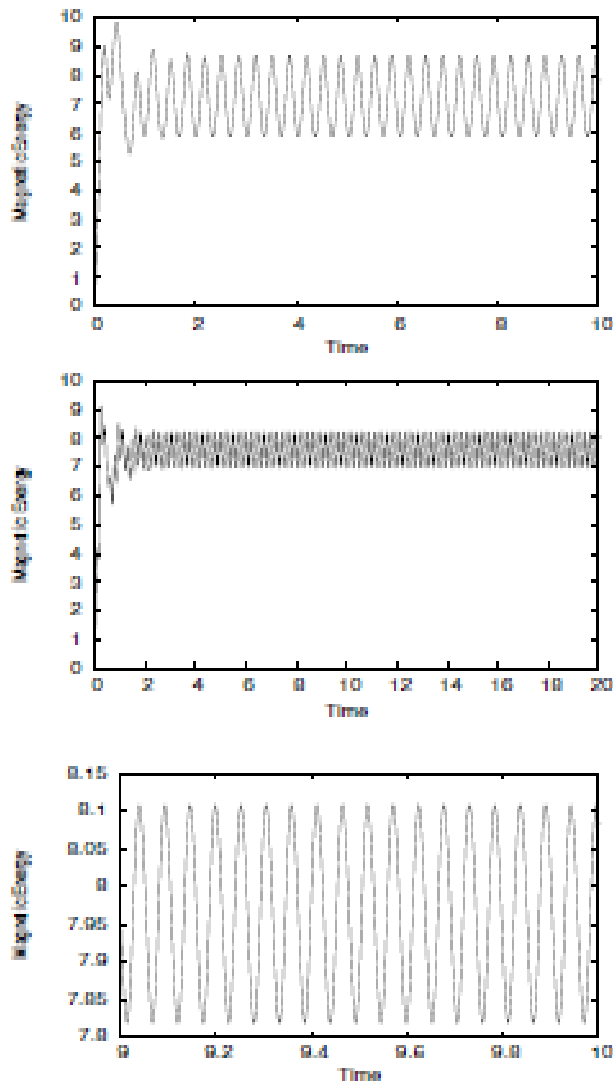


Figure 11: The magnetic energy of the nonaxisymmetric solution for $R_\omega = 25$, $R_\alpha = 20$, $b_1 = 1.0$ and $\nu_1 = 1, 18$ and 100 (right to left)

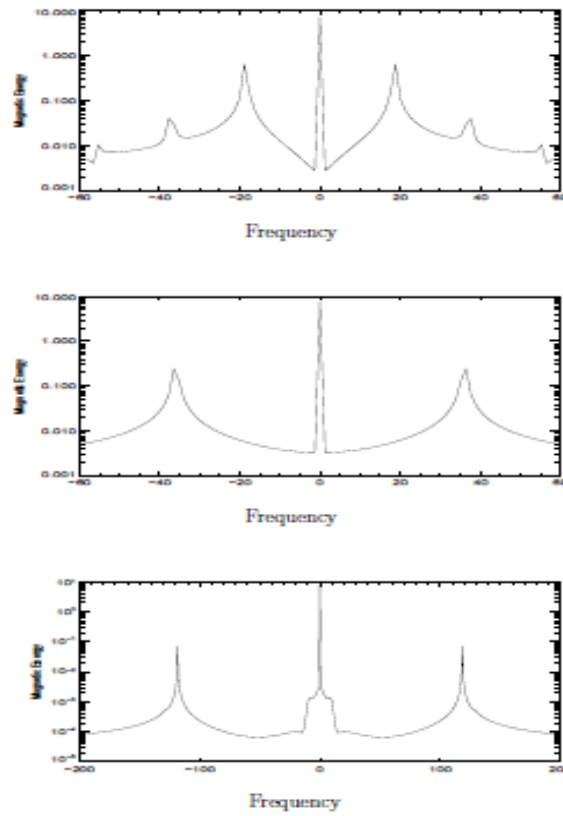


Figure 12: The Fourier transforms of the nonaxisymmetric solution at $R_\omega = 25$, $R_\alpha = 20$, $b_1 = 1.0$ and $\nu_1 = 1, 18$ and 100 (top to bottom).

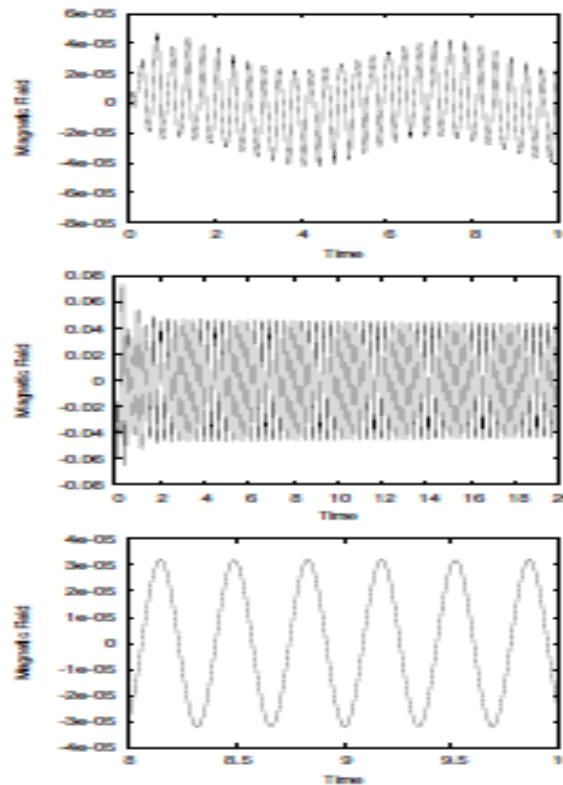


Figure 13: The magnetic fields of the nonaxisymmetric system and their Fourier transforms at $R_\omega = 25$, $R_\alpha = 20$, $b_1 = 1.0$ and $\nu_1 = 1, 18$ and 100 (top to bottom).

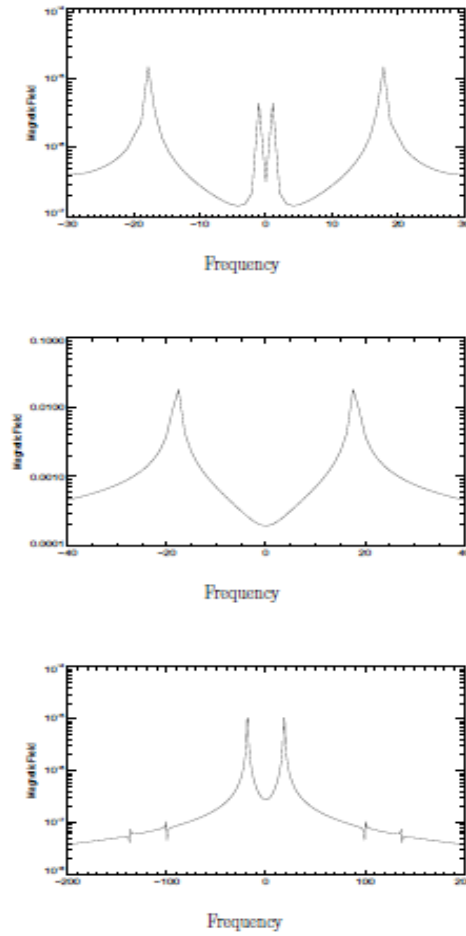


Figure 14: The Fourier transforms of the nonaxisymmetric system at $R_\omega = 25$, $R_\alpha = 20$, $b_1 = 1.0$ and $\nu_1 = 1, 18$ and 100 (top to bottom).

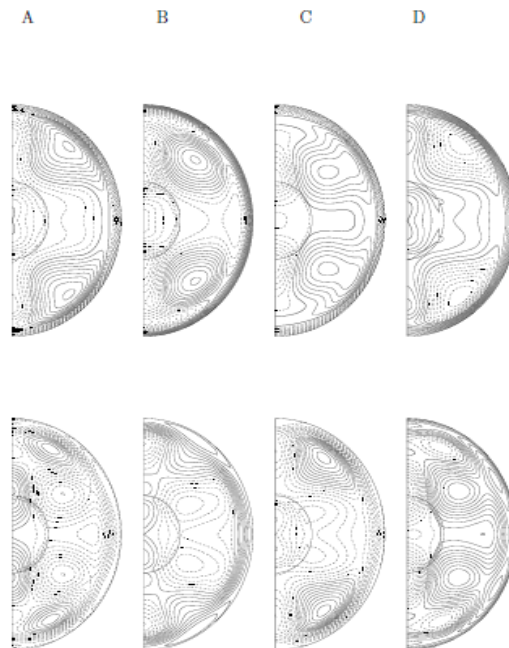


Figure 15: The rotation behaviour of the magnetic field at $R_\omega = 25$, $R_\alpha = 20$, $b_1 = 1.0$ and $\nu_1 = 100$ for the non-axisymmetric magnetic field in $\phi = 0$ (first row) and $\phi = 90$ (second row) direction at times $t = 0.01, 0.03, 0.6$ and 0.16 (for A, B, C and D respectively).

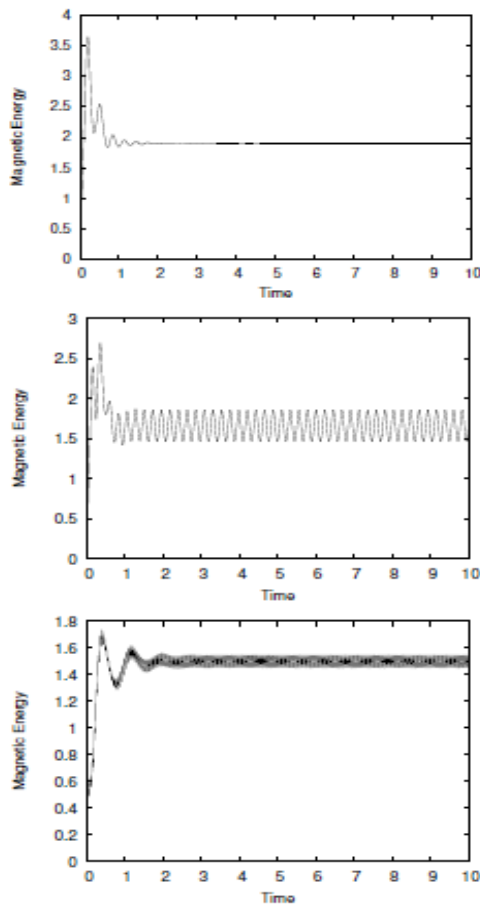


Figure 16: The non-axisymmetric magnetic energy at $R_\omega = 25$, $R_\alpha = 10$, $b_1 = 1.0$ and $v_1 = 1.0, 10$ and 100 (top to bottom).

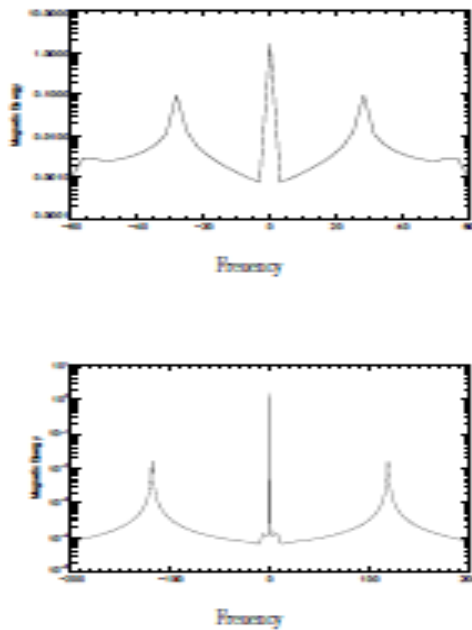


Figure 17: The Fourier transform of the magnetic energy for the nonaxisymmetric solutions at $R_\omega = 25$, $R_\alpha = 10$, $b_1 = 1.0$ and $v_1 = 10$ (top) and 100 (bottom).

Acknowledgements

I would like to thank Sarson G., Shukurov A. and Barenghi C. F. for comments on an early draft.

References

- [1]. Barenghi C.F. 1993, *Geophys. Astrophys. FluidDynamics*, 71, 163–185
- [2]. Bigazzi A. Ruzmaikin A. 2004, *The AstrophysicalJournal*, 604, 944–959.
- [3]. Brandenburg A., Krause F, Moss, D., & Tuominen I. 1989a, *A&A*, 213, 411
- [4]. Darah A. A., & Sarson G. R. 2007, *Astron. Nach.*, 328, 25–35.
- [5]. Frean D. R. 2004, *The Geodynamo*, appears in Dormy, E. (ed), *athematical Aspects of Natural Dynamos*, EDPSciences, Les Ulis.
- [6]. Gubbins D., Barber C. N., Gibbons S., & Love J. J. 2000, *Proc. R. Soc. Lond.*, 456, 1669–1683.
- [7]. Gubbins D., & Zhang K. 1994, *Phys. Earth Planet. Inter.*, 75, 225–241.
- [8]. Hollerbach R., & Jones C.A. 1993, *Nature.*, 365, 541
- [9]. Krause F. 1971, *Astron. Nachr.*, 293, 187.
- [10]. Kivelson M. G., et al. 1996a, *Nature*, 384, 537–541.
- [11]. Kivelson M. G., et al. 1996b, *Science*, 273, 337–340.
- [12]. Kivelson M. G., et al. 1996c, *Science*, 274, 396–398.
- [13]. Jones C. A., Longbottom A. W., & Hollerbach R. 1995, *Phy. Earth Planet. Inter.*, 49, 45–55
- [14]. Levy E. H. 1979, *Proc. Lunar. Planet. Sci. Conf.*, 10, 2335–2342
- [15]. Moss D. 1999, *Mon. Not. R. astr. Soc.*, 306, 300–306.
- [16]. Moss D., & Shukurov, A. 2001, *A&A*, 372, 1048–1063
- [17]. Moss D., & Shukurov, A. 2004, *A&A*, 413, 403–414
- [18]. Rädler K. H. 1989, *Fluid Dynamics*, 49, 45–55.
- [19]. Rädler K. H. 1975, *Mem. Soc. R. Sc. Liege. VIII*, 109
- [20]. Robert P. H., & Stix M. 1972, *A&A*, 18, 453.
- [21]. Starchenko S. V. 1993, *Cosmic Dynamo, Iss*, 157, 263–267.
- [22]. Sarson G. R., Jones C. A., Zhang K., & Schubert G. 1997, *Science*, 276, 1106.
- [23]. Sarson G. R., Jones C. A., & Zhang K. 1999, *Phy. Earth Planet. Inter.*, 111, 47–68
- [24]. Stix M. 1971, *A&A*, 13, 203.

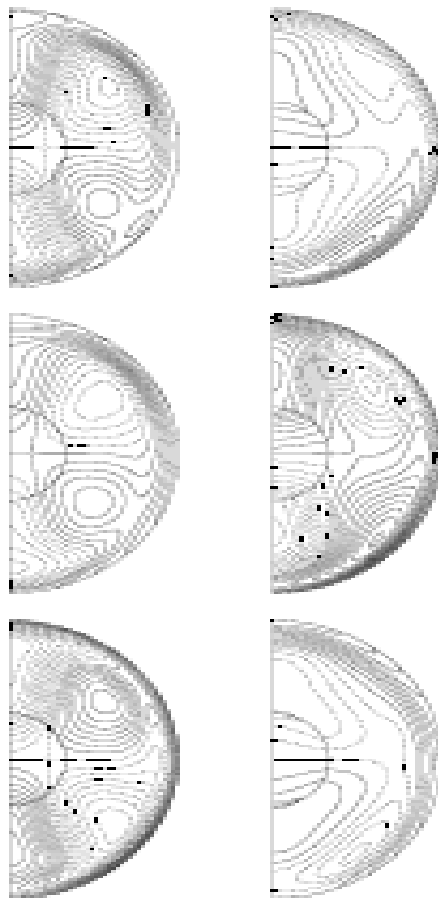


Figure 18: The rotation behaviour of the magnetic field at $R_\omega = 25$, $R_\alpha = 10$, $b_1 = 1.0$ and $v_1 = 100$, for the non-axisymmetric magnetic field in $\phi = 0$ (A) and $\phi = 90$ (B) at times $t = 10, .36, 10,42$ and $10,72$ (top to bottom).